Available online at www.sciencedirect.com
SCIENCE DIRECT®
International Journal of Thermal Sciences 44 (2005) 966–972
International Journal of Thermal Sciences
www.elsevier.com/locate/ijts

Identification of the upward gas flow velocity and of the geometric characteristics of a flame with a specific thermal sensor

K. Chetehouna [a,*], O. Séro-Guillaume [b], A. Degiovanni [b]

[a] *Laboratoire energétique explosions structures, ENSIB, 10 boulevard Lahitolle, 18020 Bourges cedex, France*
[b] *Laboratoire d'Energétique et de mécanique théorique et appliquée, CNRS-UMR 7563, ENSEM-INPL, 02 avenue de la forêt de Haye, BP 160, 54504 Vandoeuvre cedex, France*

Received 1 April 2004; received in revised form 13 November 2004; accepted 4 March 2005

Available online 15 April 2005

Abstract

The determination of the characteristics of the flame and of the upward gas flow velocity in the flames is very useful for combustion and forest fire modelling. In this paper, we intend to show that this velocity can be measured by a specific thermal sensor using a flame model. Two flame models have been considered but the fire front has been considered as a plane moving at a constant rate of spread and characterised by some geometric and physical parameters. These characteristics of the flame have been identified from experiments with the inverse method. Very similar values were obtained by the two models. The upward gas flow velocity has also been deduced using a least-squares regression based on the values of the parameters of the flame.

Keywords: Thermal sensor; Fire experiments; Flame models; Radiative heat flux; Upward gas flow velocity; Geometric characteristics of flame

1. Introduction

One of the objectives of this work is to provide one of the types of sensors that have been designed to measure thermal fields during fire experiments. A typical size for such kinds of experiments is fifty meters (size of the plot to be burnt) and it is difficult to design an apparatus giving thermal information for such a scale. The main idea is to replace the local measurements, such as those given by thermocouples for example, by the global flux measurements. We have then designed [1] a differential fluxmeter which measures the radiative flux in four horizontal directions. The other aim of this paper is to show how this device can be used to identify the geometric characteristics of flame models and can provide the upward gas flow velocity. Identification has been made with laboratory experiments in a wind tunnel with real vegetation (*Quercus coccifera*) for a line fire front.

The second section is devoted to the presentation of a designed specific thermal sensor. In the third section the two flame models will be described. We will consider the flame as a plane characterised by some physical and geometric parameters and moving at a constant rate of spread. The last section is devoted to the identification of the characteristics of the flame and the upward gas flow velocity by inverse method.

2. Description of the thermal sensor

In order to determine the characteristics of the flame, a thermal sensor has been designed, see [1] for more details. To monitor real fires, this sensor should satisfy some conditions:

- Its installation and use must be simple and convenient.
- It must be as cheap as possible.
- It should not be destroyed by the passage of the flames.

* Corresponding author. Tel.: +33 248 484 067, fax: +33 248 484 040.
E-mail address: khaled.chetehouna@ensi-bourges.fr (K. Chetehouna).

1290-0729/$ – see front matter
doi:10.1016/j.ijthermalsci.2005.03.002

Nomenclature

B	Stefan Boltzman constant
C_{co}	capacity of copper plate
C_1, C_2, C_3	positions of sensors
Fr	Froude number, $= V_{\text{wind}}^2/gh_f$
g	acceleration due to gravity
$\widehat{R}$, R_{e_1}	thermal resistance
R_i	instantaneous velocity
h_f	flame height
h_f^0	flame height without wind
R	rate of spread
S	objective function
Δt_{iTC}	time separating two successive temperature peaks
$[t_0, t_f]$	time interval when the rate of spread is constant
T_f	flame temperature
T_i	temperature of copper plate
V_{wind}	wind speed
v_{gas}	upward gas flow velocity
W	half the width of the combustion vat

Greek symbols

$\varphi_{\text{co}}, \varphi_i$	heat flux received by copper plate
θ_{co}	copper plate temperature
θ_{ste}	steel frame temperature
α_f	flame tilt angle
φ_0	emitted power of flame
β	vector of flame parameters
α_1, α_2	weighting coefficients

- Its scale must be adapted to the one used in physical models of propagation [2,3].
- If possible, it can allow an average evaluation of the radiative flux, the convective flux, the temperature of gases and their velocity.

The so-called simple thermal sensor is made of a steel frame, a thermal insulating sheet, glue sheets, 4 small copper plates and 9 thermocouples of type K, see Fig. 1.

The transfer function that gives the heat flux received by the copper plate φ_{co} as a function of the measured temperature of the plate θ_{co}, can be written:

$$\varphi_{\text{co}} = C_{\text{co}}\frac{\mathrm{d}\theta_{\text{co}}}{\mathrm{d}t} + \left(\frac{1}{\widehat{R}} + \frac{1}{R_{e_1}}\right)\theta_{\text{co}} - \frac{1}{\widehat{R}}\theta_{\text{ste}} \tag{1}$$

where C_{co} is the capacity of the copper plate, $\widehat{R}$ is a thermal resistance modelling the contact between the copper plate and the steel frame, R_{e_1} models the heat transfer between the sensor and the outside and θ_{ste} is the steel frame temperature. The different parameters involved in the transfer function have been obtained from calibration experiments, see [1].

3. Flame models and heat fluxes received by the sensor

3.1. Model I

The thermal sensor, described above, is placed at a fixed point **M** on the top of vegetation, see Fig. 2. In the first model the flame is considered as a plane surface, characterised by a height h_f, a tilt angle α_f, an emitted power φ_0, and is supposed to move at the constant rate of spread R, see [4–6].

We suppose that the sensor, the ambient air and the flame form a black enclosure. The radiative exchange between these media is approximated by an exchange between isothermal black surfaces. Therefore the radiative heat fluxes φ_i measured by the three plates of the sensor can be written, see [7]:

$$\varphi_i = B\sum_{j=1}^{3}\left(T_j^4 - T_i^4\right)F_{i-j} \tag{2}$$

In this relation, $j = 1$ (or $j = f$) indicates the flame, $j = 2$ (or $j = a$) indicates the ambient air, and $j = 3$ (or $j = i$) indicates the different plates of the sensor (plates n°1, n°2 and

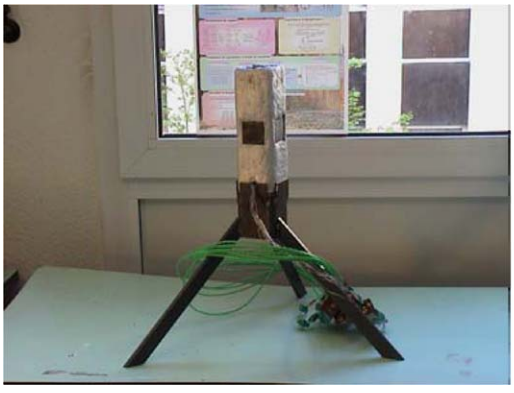

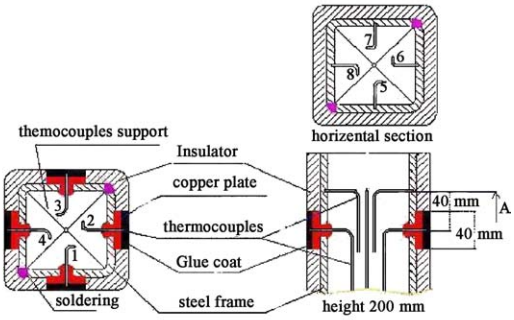

Fig. 1. Photograph and diagram of the simple sensor.

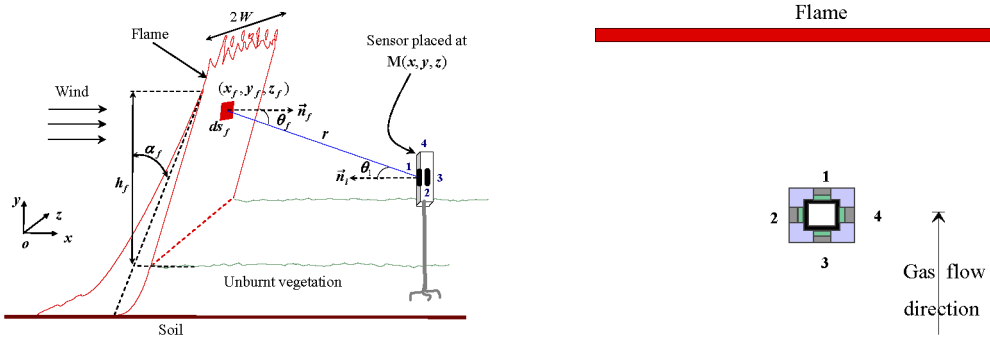

Fig. 2. Diagram of the sensor-flame system.

n° 4). B is Stefan Boltzman's constant, T_j the temperature of medium j, T_i the temperature of plate n°i and F_{i-j} the view factor between this plate and medium j.

For a complete enclosure, $\sum_{j=1}^{3} F_{i-j} = 1$, so that the radiative heat fluxes φ_i take the following form:

$$\varphi_i(t, h_f, \alpha_f, \varphi_0, R) = F_{i-f}(t, h_f, \alpha_f, R)\varphi_0\left[1 - \left(\frac{T_i}{T_f}\right)^4\right] - B\left[1 - F_{i-f}(t, h_f, \alpha_f, R)\right]\left((T_i)^4 - (T_a)^4\right) \quad (3)$$

where $\varphi_0 = BT_f^4$ is the emitted power of flame.

The view factor between plate n° i and the flame, F_{i-f} is given as

$$F_{i-f} = \int_{S_f} \frac{\cos\theta_f \cos\theta_i}{\pi r^2} \mathrm{d}s_f \quad (4)$$

with S_f the flame surface and $\mathrm{d}s_f$ its element. θ_f is the angle between the normal of $\mathrm{d}s_f$ and r, θ_i is the angle between r and the normal of plate n°i, and r is the distance between the flame and the sensor, see Fig. 2.

Calculation of the above integral leads to:

$$F_{1-f}(t, h_f, \alpha_f, R) = \frac{1}{\pi}\int_{-W}^{W}\int_{0}^{h_f} \frac{(x - x_f)[(x - x_f) - (y - y_f)\tan\alpha_f]}{((x - x_f)^2 + (y - y_f)^2 + (z - z_f)^2)^2} \times \mathrm{d}y_f\,\mathrm{d}z_f \quad (5)$$

$$F_{2-f}(t, h_f, \alpha_f, R) = \frac{1}{\pi}\int_{-W}^{z}\int_{0}^{h_f} \frac{(z - z_f)[(x - x_f) - (y - y_f)\tan\alpha_f}{((x - x_f)^2 + (y - y_f)^2 + (z - z_f)^2)^2} \times \mathrm{d}y_f\,\mathrm{d}z_f \quad (6)$$

$$F_{4-f}(t, h_f, \alpha_f, R) = \frac{1}{\pi}\int_{z}^{W}\int_{0}^{h_f} \frac{(z - z_f)[(x - x_f) - (y - y_f)\tan\alpha_f}{((x - x_f)^2 + (y - y_f)^2 + (z - z_f)^2)^2} \times \mathrm{d}y_f\,\mathrm{d}z_f \quad (7)$$

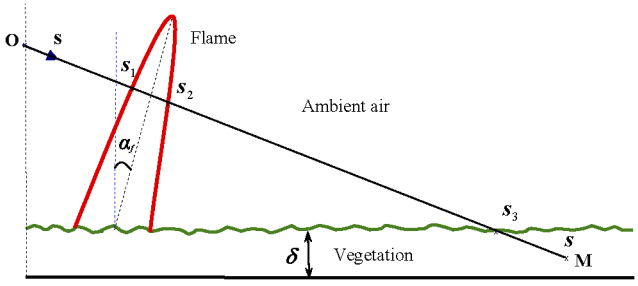

Fig. 3. Geometry for integration of radiative transfer equation.

where $x_f = Rt + y_f \tan(\alpha_f)$ is the abscissa of the flame, W is half the width of the combustion vat.

When the sensor is outside the flame, temperature T_i is negligible compared to the temperature of the flame T_f, so that relation (3) can be written:

$$\varphi_i(t, h_f, \alpha_f, \varphi_0, R) = F_{i-f}(t, h_f, \alpha_f, R)\varphi_0 - B\left[1 - F_{i-f}(t, h_f, \alpha_f, R)\right]\left((T_i^r)^4 - (T_a)^4\right) \quad (8)$$

3.2. Model II

Another model based on an approximate resolution of the radiative transfer equation (see [7]) can be considered, as is explained below. We must calculate the heat flux from the flame to the different faces of the sensor. Let us consider a point **M** inside or just above the vegetation. A line **OM** crosses the flame in s_1, s_2 and the top of the vegetation in s_3, see Fig. 3.

The different radiation coefficients are supposed to be constant (ambient air, flame, vegetation) and the scattering coefficient is supposed to be null, see [8,9], so that the extinction coefficient takes the following values:

(i) In $[o, s_1]$, $K = K_{\text{air}} = 0$.
(ii) In $[s_1, s_2]$, $K = K_f$.
(iii) In $[s_2, s_3]$, $K = K_{\text{air}} = 0$.
(iv) In $[s_3, s]$, $K = K_v$.

The radiative intensity at point s is then:

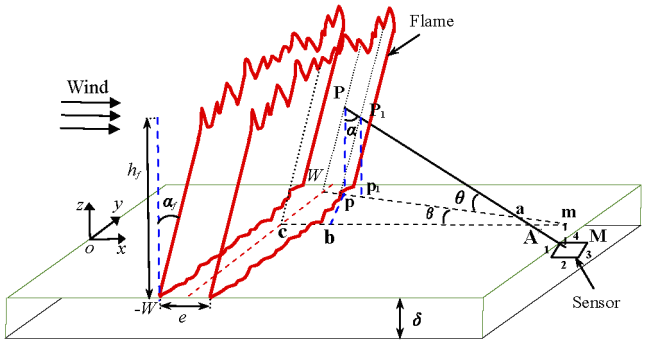

Fig. 4. Positions of the sensor and the flame.

$$i(s) = K_f e^{-K_v(s-s_3)} \int_{s_1}^{s_2} i_b(\bar{s}) e^{-K_f(s_2-\bar{s})}\,\mathrm{d}\bar{s} + K_v \int_{s_3}^{s} i_b(\bar{s}) e^{-K_v(s-\bar{s})}\,\mathrm{d}\bar{s} \tag{9}$$

with $i_b(\bar{s}) = \frac{BT_f^4}{\pi}$ in $[s_1, s_2]$ and $i_b(\bar{s}) = \frac{BT_v^4}{\pi}$ in $[s_3, s]$. Then if we assume that the flame is thin, see [10], the expression (9) becomes:

$$i(s) = K_f \frac{BT_f^4}{\pi} e^{-K_v(s-s_3)} \int_{s_1}^{s_2} \mathrm{d}\bar{s} + K_v \int_{s_3}^{s} i_b(\bar{s}) e^{-K_v(s-\bar{s})}\,\mathrm{d}\bar{s} \tag{10}$$

The radiative heat flux received by surface n°i of the sensor with unit normal $\mathbf{n}_i$ is:

$$\varphi_i(\mathbf{M}) = \int_{\omega=0}^{4\pi} i(s)\mathbf{s}\cdot\mathbf{n}_i\,\mathrm{d}\omega \tag{11}$$

where $\mathrm{d}\omega$ is the elementary solid angle in the direction $\mathbf{s}$.

Let us now consider the situation of the experiments. The flame is supposed to be inclined with an angle α_f, its height, its thickness and its width are respectively h_f, e and $2W$, see Fig. 4.

The projections of the points $\mathbf{P}$, $\mathbf{P}_1$ and $\mathbf{M}$ on the top surface of the vegetation are denoted $\mathbf{p}$, $\mathbf{p}_1$ and $\mathbf{m}$. The useful distances are denoted $\rho = \mathbf{PM}$, $\rho_0 = \mathbf{P}_1\mathbf{M}$, $r = \mathbf{pm}$, $r_0 = \mathbf{p}_1\mathbf{m}$ and $x_3 = \mathbf{mM}$. The unit vectors normal to the plates are denoted $\mathbf{n}_i$ and the unit vector $\mathbf{s}$ along direction $\mathbf{PM}$ is $\mathbf{s} = (\sin\alpha\cos\beta, -\sin\alpha\sin\beta, -\cos\alpha)$. If we insert expression (10) in (11), we obtain:

$$\varphi_i(\mathbf{M}) = K_f \frac{BT_f^4}{\pi} \int_{\omega=0}^{4\pi}\int_{s_1}^{s_2} e^{-K_v(s-s_3)}\mathbf{s}\cdot\mathbf{n}_i\,\mathrm{d}\bar{s}\,\mathrm{d}\omega + K_v \int_{\omega=0}^{4\pi}\int_{s_3}^{s} i_b(\bar{s}) e^{-K_v(s-\bar{s})}\mathbf{s}\cdot\mathbf{n}_i\,\mathrm{d}\bar{s}\,\mathrm{d}\omega \tag{12}$$

Inside the flame $\mathrm{d}\bar{s}\,\mathrm{d}\omega = \frac{\mathrm{d}\Omega}{\mathbf{PM}^2}$ with $\mathrm{d}\Omega$ being a volume element, inside the vegetation $\mathrm{d}\bar{s}\,\mathrm{d}\omega = \frac{\mathrm{d}\Omega}{\mathbf{AM}^2}$. The last term of (12) is the contribution of the vegetation to the radiative flux.

In order to characterise the flame only, this last term should be taken away. Let us notice that because we assume that the vegetal homogenised medium is isotropic, the contribution of the vegetation is the same in all directions and is given by the rear plate number 3. Then after some calculations, the flame flux can be written:

$$\varphi_i(\mathbf{M}) = \varphi_i - \varphi_3 = -K_f \frac{BT_f^4}{\pi} \int_{Rt-e/2}^{Rt+e/2} \mathrm{d}x \int \cos\beta\,\mathrm{d}\beta \times \int_{\alpha_0}^{\alpha_1} e^{-K_v \frac{x_3}{\cos\alpha}} \mathbf{s}\cdot\mathbf{n}_i\,\mathrm{d}\alpha \tag{13}$$

where R is the rate of spread,

$$\alpha_0 = \operatorname{arctag}\left(\frac{r}{x_3}\right), \qquad \alpha_1 = \operatorname{arctag}\left(\frac{r}{h_f + x_3}\right),$$

$$r = \frac{x - Rt - h_f \operatorname{tg}\alpha_f}{\cos\beta}$$

After some calculations we obtain the following expressions for the radiative heat fluxes:

Face 1 (*ahead face*):

$$\varphi_1(\mathbf{M}) = 2K_f e \frac{BT_f^4}{\pi} \int_0^{\beta_W} (\cos\alpha_1 - \cos\alpha_0)\cos^2\beta\,\mathrm{d}\beta \tag{14}$$

Faces 2 *and* 4 (*lateral faces*):

$$\varphi_2(\mathbf{M}) = \varphi_4(\mathbf{M}) = K_f e \frac{BT_f^4}{\pi} \int_0^{\beta_W} (\cos\alpha_1 - \cos\alpha_0)\sin\beta\cos\beta\,\mathrm{d}\beta \tag{15}$$

with

$$\beta_W = \operatorname{arctg}\left(\frac{W}{x_0 - Rt - h_f \operatorname{tg}\alpha_f}\right)$$

4. Objective function and optimisation method

To identify the parameters of the flame the following objective function S will be minimised:

$$S(\beta) = \int_{t_0}^{t_f} \left(\varphi_{1\exp}(t) - \varphi_1(t,\beta)\right)^2 \mathrm{d}t + \alpha_1 \int_{t_0}^{t_f} \left(\varphi_{2\exp}(t) - \varphi_2(t,\beta)\right)^2 \mathrm{d}t + \alpha_2 \int_{t_0}^{t_f} \left(\varphi_{4\exp}(t) - \varphi_4(t,\beta)\right)^2 \mathrm{d}t \tag{16}$$

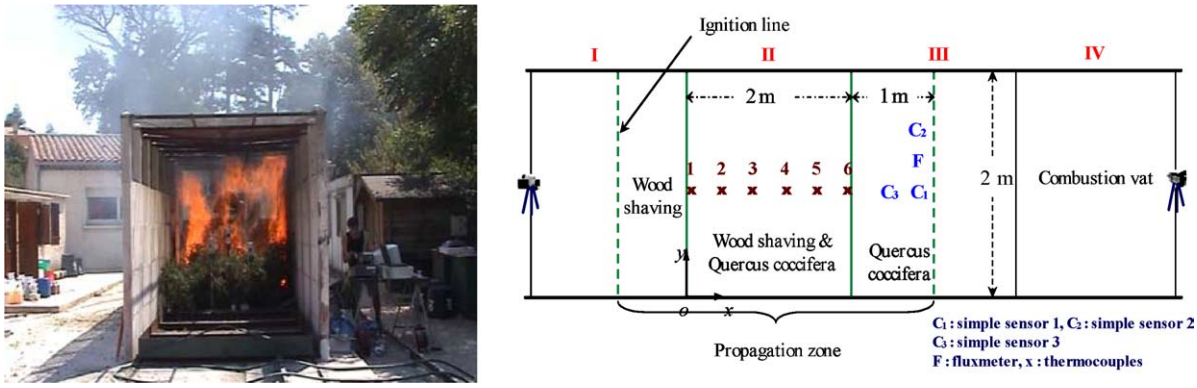

Fig. 5. Fire experiment in the B.E.S.T. tunnel.

$\varphi_{k\exp}(t)$ and $\varphi_k(t,\beta)$, $k = 1, 2, 4$ are respectively the measured values and the theoretical values of the heat fluxes. $\beta = (h_f, \alpha_f, \varphi_0, R)$ is the vector of the parameters of the flame for model I and for model II $\beta = (h_f, \alpha_f, R, T_f, K_f, e)$. $[t_0, t_f]$ is the time interval when the rate of spread is constant and α_1, α_2 are the weighting coefficients.

Looking for $\min_\beta S$, we have to solve the equations $\frac{\partial S}{\partial \beta_j} = 0$, which can be written:

$$\int_{t_0}^{t_f} \frac{\partial \varphi_1}{\partial \beta_j}\big(\varphi_{1\exp(t)} - \varphi_1(t,\beta)\big)\,\mathrm{d}t + \alpha_1 \int_{t_0}^{t_f} \frac{\partial \varphi_2}{\partial \beta_j}\big(\varphi_{2\exp}(t) - \varphi_2(t,\beta)\big)\,\mathrm{d}t + \alpha_2 \int_{t_0}^{t_f} \frac{\partial \varphi_4}{\partial \beta_j}\big(\varphi_{4\exp}(t) - \varphi_4(t,\beta)\big)\,\mathrm{d}t = 0 \qquad (17)$$

We used an algorithm based on the Newton's method. Each iteration involves the approximate solution of a large linear system using the method of preconditioned conjugate gradients (PCG).

5. Results and discussion

In a large fire tunnel, named B.E.S.T., series of fire experiments, see Fig. 5, were carried out with *Quercus coccifera* (whose height was about 1 m), a dominant vegetation in the south of France, with a load (surface density) of 3 kg·m^{-2}, see [11] for more details.

Three thermal sensors, a fluxmeter, two video cameras and six thermocouples dedicated to the determination of the rate of spread were settled. The position of the different systems is indicated in Fig. 5.

These thermal sensors were settled at position in the coordinate system *oxy*, see Fig. 5:

- C_1 (3 m, 1 m), sensor number 1 was at height 1 m, it was intended to measure the flux outside vegetation.

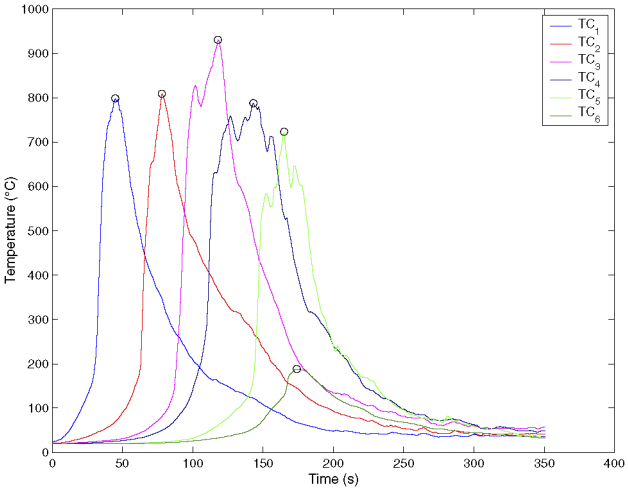

Fig. 6. Different temperatures given by the thermocouples.

- C_2 (3 m, 1.5 m), sensor number 2 was placed at height 0.8 m and was measuring the flux arriving on the vegetation.
- C_3 (2.75 m, 1 m), sensor number 3 was at height 0.6 m and was measuring the flux inside the vegetation.

The distance between the thermocouples was 40 cm so that the instantaneous velocity is given by: $R_i = 40/\Delta t_{iTC}$, Δt_{iTC} is the time separating two successive temperature peaks, see Fig. 6. The rate of spread is the average of the local rates of spread during the stationary phase.

In the present work, we only use the heat fluxes measured by the sensor placed in the middle of the tunnel at a height of 1 m above the ground. The measured heat fluxes are presented in Figs. 7 and 8.

Solving equations (17) for the two flame models leads to the results given in Table 1. The relative gap between the theoretical fluxes and those measured by the thermal sensor is between 1 and 3%.

As indicated in Table 1, the experimental values of the flame height and the rate of spread can be favourably compared to the values of the two models. The identification results of the parameters of the flame are very close in both

cases so that we can say that the identification of these parameters is insensitive to the flame model.

We can now estimate the vertical velocity of gas.

For a fire spreading across a horizontal surface under the wind effect, flame tilt angle, α_f, is the result of the competition between buoyancy and wind and we assume that α_f is given by, see [12,13]:

$$\tan(\alpha_f) = \frac{V_{\text{wind}}}{v_{\text{gas}}} \tag{18}$$

here V_{wind} and v_{gas} represent respectively the free stream wind speed and the upward gas flow velocity in still air, both at mid-flame.

Velocity v_{gas} is deduced as being the inverse of the slope of the curve $\tan(\alpha_f)$ versus V_{wind} by using a least-squares regression based on the values of the flame parameters. Fig. 9 shows this linear regression.

From the slope of this curve one can obtain the value of upward gas flow velocity $v_{\text{gas}} = 0.48\ \text{m}\cdot\text{s}^{-1}$.

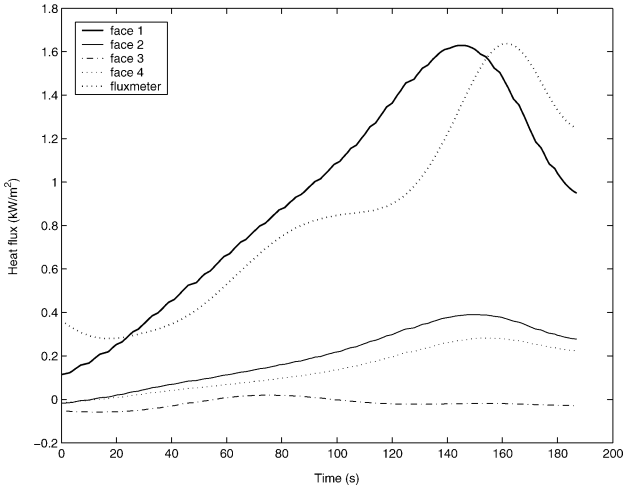

Fig. 7. Heat fluxes given by the sensor in fire experiment without wind.

With dead pine needles as fuel bed, Porterie et al. [14] have proposed the different flame heights, see Table 2.

Although there is a difference due to the nature of vegetation (dead pine needles, Quercus coccifera), the flame heights obtained by our two models seem to be close to those obtained by Porterie et al.

These authors have also presented a confrontation of literature results for the tilt angle of the flame, see Table 3. Let us notice that these values are taken for pine needles. The values obtained in the present work are greater than those presented in the literature, but the considered vege-

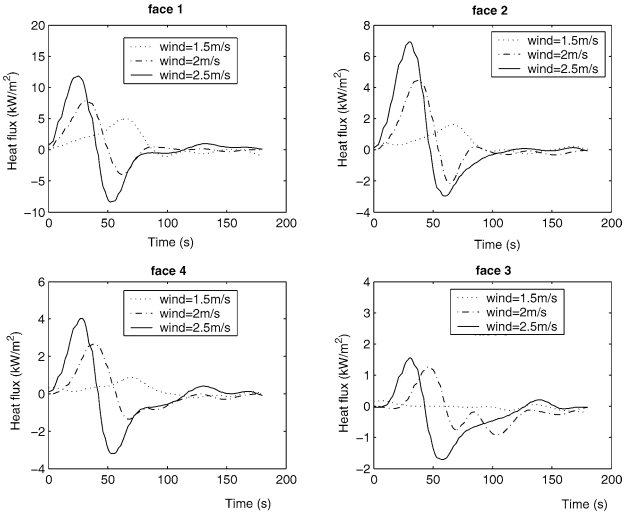

Fig. 8. Heat fluxes given by the sensor in fire experiments with winds.

Table 2
Different flame heights

Flame height (cm)			
Wind speed [m·s]	Model I	Model II	Porterie et al.
1.5	48	43	40
2	41	38	31
2.5	38	34	29

Table 1
Flame parameters for different experiments

Wind speed V_{wind} [m·s]		0	1.5	2	2.5
Experimental values	Rate of spread R [cm·s] *by thermocouples*	1.5	2.1	4	5.7
	Flame height h_f [cm] *by video camera*	160	50	40	30
Model I	Rate of spread R [cm·s]	1.7	2.2	3.9	5.6
	Flame height h_f [cm]	140	48	41	38
	Tilt angle α_f [°]	0	72	77	79
	Emitted power φ_0 [kW·m^{-2}]	5.2	11.8	14.9	18.2
Model II	Rate of spread R [cm·s]	1.7	2.4	4.2	6.0
	Flame height h_f [cm]	170	43	38	34
	Tilt angle α_f [°]	0	72	77	80
	Flame temperature T_f [°C]	807	816	1176	1180
	Extinction coefficient K_f [m^{-1}]	0.14	0.15	0.11	0.12
	Flame thickness e [cm]	35	53	54	58

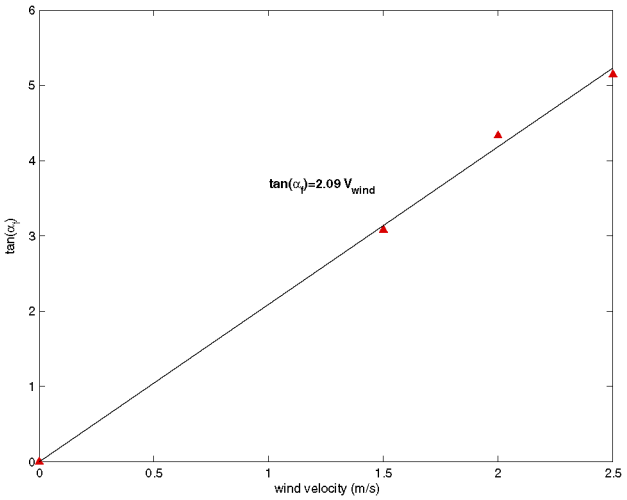

Fig. 9. Determination of upward gas flow velocity.

Table 3
Different tilt angles of flame

Tilt angle of flame (°)			
Wind speed [m·s]	Porterie et al. [14]	Albini [12]	Nelson and Adkins [15]
1.5	42	42.2	36.9
2	59.8	54.4	43.9
2.5	61.1	60	47.6

tations are different. Quercus coccifera is a not as compact as pine needles and the height is not the same. Under wind there is an air flow inside Quercus coccifera, which is probably not the case for pine needles, this flow should tilt the flame. It means that the tilting of the flame is a complex phenomenon related to the hydrodynamics in the vegetation.

6. Conclusion

The knowledge of the upward gas flow velocity in the flames is useful for forest fire modelling but it may have other applications in combustion modelling. We have seen that this velocity can be correctly determined by a correlation between wind velocity and tilt angle. Its value has been obtained within a relative error of 2%. The geometric characteristics of two flame models have been identified by the minimisation of an objective function. These models have given the radiative heat fluxes received by the thermal sensor in four horizontal directions. These fluxes have been measured during fire experiments with a real vegetation.

However, very similar values for flame parameters were observed on the two models.

At least, let us notice that the sensor briefly presented here has other applications in forest fire modelling. It has been used for the measurements of radiative absorption coefficient, the calibration of vegetation flame models and the reconstruction of the fire front.

Acknowledgement

This research has been done under the support of European community, research contract “SPREAD” n° EVG1-CT-2001-00043.

References

[1] K. Chetehouna, O. Séro-Guillaume, A. Degiovanni, Study of a thermal sensor intended for the calibration of propagation models of forest fires, in: Proceedings of Inverse Problems and Experimental Design in Thermal and Mechanical Engineering, Eurotherm Seminar 68, Edizioni Ets Poitiers, France, 2001, pp. 287–292.
[2] R.-O. Weber, Modelling fire spread through fuel beds, Prog. Energy Combust. Sci. 17 (1991) 67–82.
[3] J. Margerit, O. Séro-Guillaume, Modelling forest fires. Part II: reduction to two-dimensional models and simulation of propagation, Internat J. Heat Mass Transfer 45 (8) (2002) 1723–1737.
[4] J.-L. Dupuy, Testing two radiative physical models for fire spread through porous forest fuel beds, Combust. Sci. Technol. 155 (2000) 149–180.
[5] R.-O. Weber, Analytical models for fire spread due to radiation, Combust. Flame 78 (1989) 398–408.
[6] N.-J. De Mestre, E.-A. Catchpole, D.-H. Anderson, R.-C. Rothermel, Uniform propagation of a planar fire front without wind, Combust. Sci. Technol. 65 (1989) 231–244.
[7] R. Siegel, J. Howell, Thermal Radiation Heat Transfer, fourth ed., Taylor & Francis, New York, 2002.
[8] F.-A. Albini, Wildland fire spread by radiation: A model including fuel cooling by convection, Combust. Sci. Technol. 45 (1985) 101–113.
[9] K. Chetehouna, M. Er-Riani, O. Séro-Guillaume, On the rate of spread for some reaction–diffusion models of forest fire propagation, Numer. Heat Transfer Part A 46 (8) (2004) 765–784.
[10] L. Ferragut, I. Asensio, S. Monedero, Modelling slope, wind and moisture content effects on fire spread, in: European Congress on Computational Methods in Applied Sciences and Engineering ECCOMAS, Jyväskylä, 24–28 July 2004.
[11] K. Chetehouna, Contribution à la métrologie des feux de végétation, Ph.D. Thesis, Institut National Polytechnique de Lorraine, France, 2002.
[12] F.-A. Albini, A model for the wind-blown flame from a line fire, Combust. Flame 43 (1981) 155–174.
[13] F. Morandini, P.-A. Santoni, J.-H. Balbi, The contribution of radiant heat transfer to laboratory-scale fire spread under the influence of wind and slope, Fire Safety J. 36 (2001) 519–543.
[14] B. Porterie, D. Morvan, J.-C. Loraud, M. Larini, Firespread through fuel beds: Modeling of wind-aided fires and induced hydrodynamics, Phys. Fluids 12 (7) (2000) 1762–1782.
[15] R.-M. Nelson, C.-W. Adkins, Flame characteristics of wind-driven surface fires, Canad. J. Forest Res. 16 (1986) 1293.